Edge Preserving Regularization and Tracking for Diffusion Tensor Imaging

Klaus Hahn[1], Sergei Prigarin[2], and Benno Pütz[3]

[1] Institute of Biomathematics and Biometrics of the National Research Center for Environment and Health — GSF — , Postfach 1129, D–85758 Neuherberg, Germany
hahn@gsf.de
[2] Institute of Computational Mathematics and Mathematical Geophysics, Novosibirsk, Russia
smp@osmf.sscc.ru
[3] Max-Planck-Institute of Psychiatry, München, Germany
puetz@mpipsykl.mpg.de

Abstract. Two major problems in MR Diffusion Tensor Imaging, regularization and tracking are addressed. Regularization is performed on a variance homogenizing transformation of the tensor field via a nonlinear filter chain to preserve discontinuities. The suitability of the smoothing procedure is validated by Monte Carlo simulations. For tracking, the tensor field is diagonalized and a local bilinear interpolation of the corresponding direction field is performed. The track curves, which are not restricted to the measured grid, are modeled by following stepwise the interpolated directions. The presented methods are illustrated by applications to measured data.

1 Introduction

Diffusion Tensor Imaging, which can appreciably contribute to explore anatomical connectivity, recently became a main topic in human brain mapping. Two essential problems on the way to detect the flow of axon fibers are discussed in this paper: Improvement of the low signal to noise ratio in the tensor field via regularization and modeling of the axon bundle flow.

Regularization or, equivalently, smoothing including convenient priors is essential for the quantification of anisotropy and direction of the diffusion field as convenient measures are biased by low signal to noise ratio [1,2]. Smoothing can be performed on different levels of description for the direction field, e. g., on the diffusion weighted images of the measured signal [3], on the tensor field [4] or on the vector field of the main diffusion directions [5]. Our approach regularizes a variance homogenizing transformation of the tensor field, as the noise variance of the tensor field is strongly dependent on measuring parameters and the field amplitude. The signals in the tensor field show discontinuous patterns, due to tissue or organ dependent changes in the anisotropy of diffusion. Therefore, an edge preserving smoother which does not blur the field is applied. A validation of this smoothing method is performed by a Monte Carlo simulation

W. Niessen and M. Viergever (Eds.): MICCAI 2001, LNCS 2208, pp. 195–203, 2001.

via the Stejskal-Tanner equations [6]. Our smoothing procedure concerns the increase of signal to noise ratio on the measurement grid, so it concerns averaged properties of the actual axon flow. Tracking on the other hand is regarded as a way to model this flow below the grid scale. To achieve this, the smoothed tensor field is diagonalized and the direction field of the principal eigenvectors is further analyzed. For a given seed point in white matter, not necessarily on the grid, the track of axon fibers is modeled. To do this, the direction field is interpolated locally by a bilinear procedure, then the track is followed by differential equation discretization. The method is applied to real data and results concerning the corpus callosum region are presented. The diffusion tensor images were acquired on a 1.5 T clinical scanner (Signa Echospeed, GE) using a diffusion weighted EPI sequence with 6 non-collinear gradient orientations and 4 b-factors, $b_{\max}$=880 s/mm^2. 24 contiguous slices with a spatial resolution of $1.875\times1.875\times3\,\mathrm{mm}^3$ were acquired.

2 Edge Preserving Regularization of the Diffusion Tensor Field

Our approach to regularization or smoothing is similar to that of Basser et al. [4], as we are essentially smoothing the tensor field [7]. However, in contrast to Basser et al., who use linear B-Spline approximation which gives blurring of the resulting fields, we use nonlinear filters which are edge preserving and homogenizing, as the measured fields show clear discontinuities and as the curvature of the direction field should be small [5]. This smoothing technique differs from that used by Parker et al [3], who use the "Perona Malik-variant" of the diffusion equation. We use a chain of three dimensional nonlinear Sigma filters, the "Aurich-chain" [8], which is easy to implement and has suitable numerical and statistical properties.

According to the exponential behavior of the Stejskal-Tanner equations [9,1,2],

$$F_I^b(\boldsymbol{x})/F^0(\boldsymbol{x}) = \exp(-b\hat{\boldsymbol{G}}_I^T * D(\boldsymbol{x}) * \hat{\boldsymbol{G}}_I) \tag{1}$$

where $D(\boldsymbol{x})$ is the spatial tensor field, $F_I^b(\boldsymbol{x}) = |Signal_I^b(\boldsymbol{x}) + n_{\mathrm{Re}} + in_{\mathrm{Im}}|$ with n_{Re}, $n_{\mathrm{Im}} \in N(0,\sigma)$, $F^0(\boldsymbol{x})$ is the T_2-weighted field, $b > 0$ is the diffusion weighting parameter, and $\hat{\boldsymbol{G}}_I, I = 1,\ldots,6$ are normalized gradient vectors. For high b-values the variance of the noise in the tensor field $D(\boldsymbol{x})$ depends strongly on the amplitude, see Fig. 1 for one dimensional simulated examples. Therefore, to achieve noise homogeneity, an important prior condition for smoothing by filters, filtering should not be performed on the coefficients D_{xx}, D_{xy}, etc. of the symmetric $D(\boldsymbol{x})$ matrix directly but on it's exponential, e. g. on $f = \exp(-bD_{xx}(\boldsymbol{x}))$.

The fields in Eq. (1) show discontinuities, which are due to voxel wise changes in diffusion anisotropy (caused, e. g., by tissue dependent anisotropy or by fiber crossing creating partial volume effects), see Fig. 2, Panel A. Therefore, nonlinear edge preserving filtering is applied. For every field f the "Aurich-chain" is formulated in three dimensions according to:

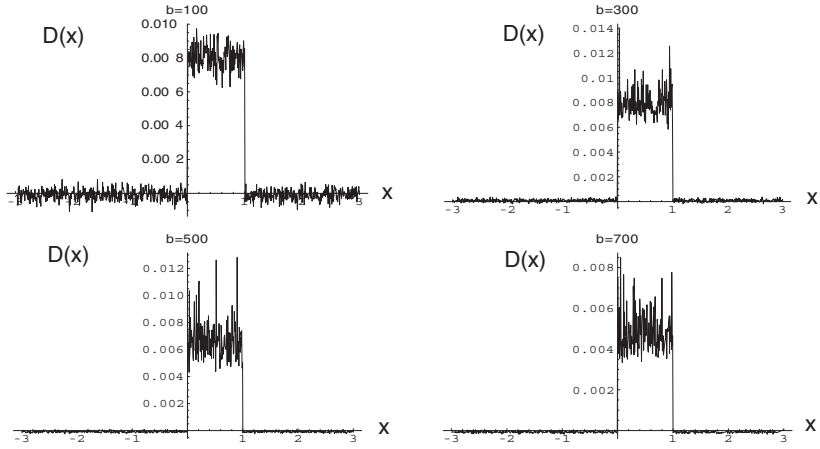

Fig. 1: A smooth tensor coefficient $D(x)$ for one space dimension is assumed as a step function. According to theMonte Carlo simulation described in text $\sigma = 0.03F^0$ complex Gaussian noise is added to the Signal and $D(x)$ is plotted for b=100, 300, 500, and 700 s/mm^2. The variance depends strongly on b and on the amplitude of the field

$$
\begin{aligned}
f(\boldsymbol{x})_{\text{new}} &= \sum_{\boldsymbol{y}\in\text{Neighborhood}(\boldsymbol{x})} \exp\left(-\frac{(\boldsymbol{x}-\boldsymbol{y})^2}{2\sigma^2}\right)\exp\left(-\frac{(f(\boldsymbol{x})-f(\boldsymbol{y}))^2}{2\tau^2}\right)\frac{f(\boldsymbol{y})}{Norm} \\
&= F_\sigma^\tau \circ f(\boldsymbol{x}) \\
Norm &= \sum_{\boldsymbol{y}\in\text{Neighborhood}(\boldsymbol{x})} \exp\left(-\frac{(\boldsymbol{x}-\boldsymbol{y})^2}{2\sigma^2}\right)\exp\left(-\frac{(f(\boldsymbol{x})-f(\boldsymbol{y}))^2}{2\tau^2}\right) \qquad (2) \\
f(\boldsymbol{x})_{\text{smooth}} &= F_{\sigma*1.59*1.59}^{(\tau/3)/2} \circ F_{\sigma*1.59}^{\tau/3} \circ F_\sigma^\tau \circ f(\boldsymbol{x}) \quad ,
\end{aligned}
$$

where σ is the voxel width and τ is three times an estimate of the smallest step in the field f which should be preserved. A lower bound of this step is given by the standard deviation of the noise in f.

This algorithm is statistically robust with respect to noise details (deviations from independent Gaussian noise), numerically stable, and computationally fast, as tabulation methods can be used. See [10] for further details and for a review of recent edge preserving smoothers. In Fig. 2, Panel B, some tensor coefficients of the smoothed field are shown, three iterations in the chain gave a suitable flatness of the resulting field, which is equivalent to a low curvature in the direction field.

In addition, to demonstrate the quality of our filter method, a validation based on Monte Carlo simulation was performed. The smoothed three dimensional tensor data around the corpus callosum which are partially shown in Fig. 2, Panel B, were used as reference. By Eq. (1) they were corrupted with noise via the following steps: Assume F^0=1000 and derive via Eq. (1) $Signal_I^b(\boldsymbol{x})$, for b=100, 300, 500, and 700 s/mm^2 and $\hat{\boldsymbol{G}}_1 = (1,0,0)$, $\hat{\boldsymbol{G}}_2 = (0,1,0)$, $\hat{\boldsymbol{G}}_3 = (0,0,1)$, $\hat{\boldsymbol{G}}_4 = (1/\sqrt{2}, 1/\sqrt{2}, 0)$, $\hat{\boldsymbol{G}}_5 = (1/\sqrt{2}, 0, 1/\sqrt{2})$, and $\hat{\boldsymbol{G}}_6 = (0, 1/\sqrt{2}, 1/\sqrt{2})$. These

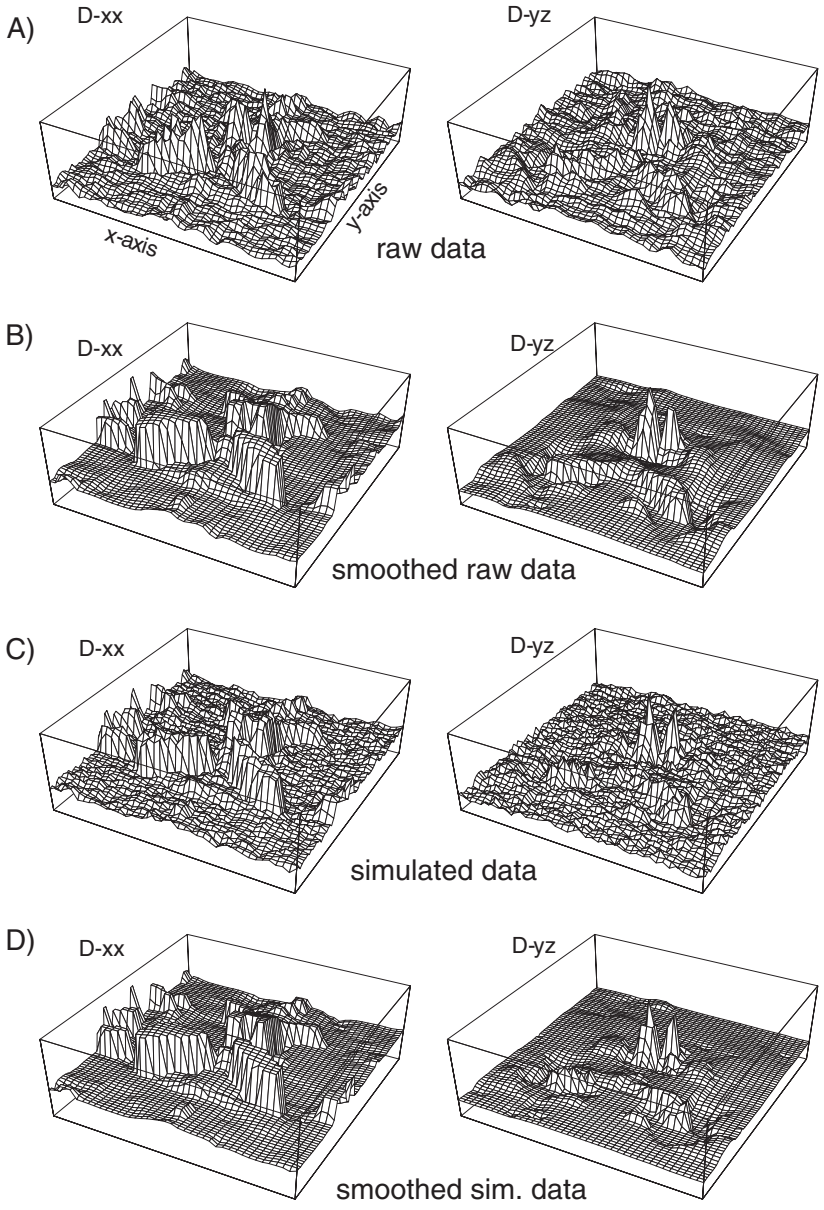

Fig. 2: In Panel A, axial slices of $D_{xx}(\boldsymbol{x})$ and $D_{yz}(\boldsymbol{x})$ for identical regions around the corpus callosum are shown for raw data. Panel B presents the corresponding smoothed fields. Panel C shows the noise corrupted fields of Panel B, see Monte Carlo simulation in text for details. Panel D demonstrates that the applied smoother indeed reproduces Panel B with high precision

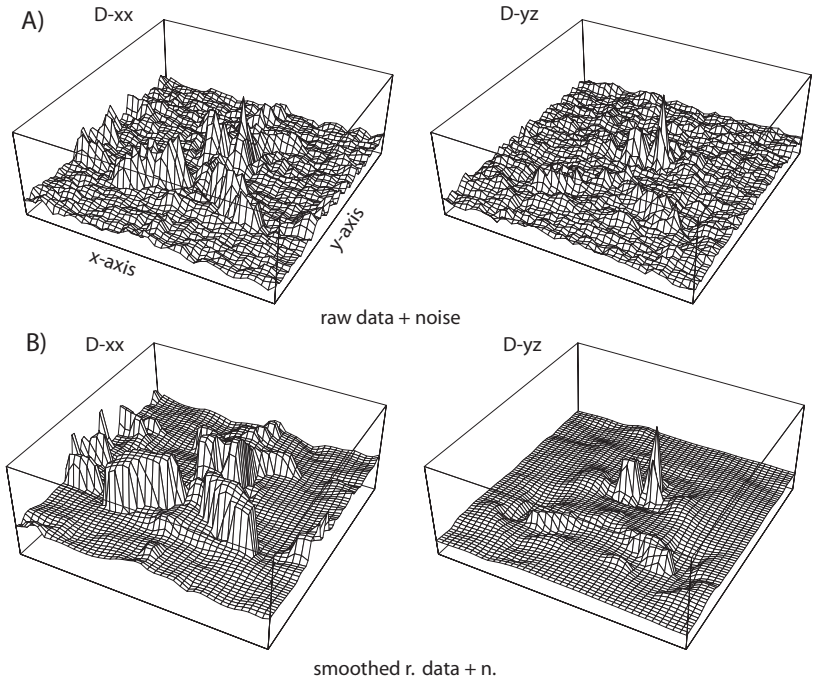

Fig. 3: Effect of the robust smoother on tensor coefficients (as in Fig. 2)

25 fields, including F^0, were then corrupted by complex Gaussian noise, $N(0, \sigma)$, with σ=3% of $F^0(\boldsymbol{x})$. The corresponding tensor field $D(\boldsymbol{x})$ was calculated at every space point via multivariate linear regression. This regression comprised all 24 linear equations corresponding to the logarithmic variant of Eq. (1) for the four b-values. Some coefficients of the resulting noisy tensor field $D(\boldsymbol{x})$ are shown in Fig. 2, Panel C. Smoothing of $D(\boldsymbol{x})$ was performed in the same way as for the raw data, using b=400 s/mm^2 in the exponential transformation, with results shown in Fig. 2, Panel D. The good agreement with the reference in Panel B demonstrates the suitability of the applied filter method. In a second test the raw data signals of Fig. 2, Panel A were additionally corrupted by adding the noise of Panel C, as shown in Fig. 3, Panel A. An application of the filter chain demonstrates the robustness of the method as seen in Fig. 3, Panel B.

3 Tracking

To derive the main diffusion directions of the axon bundles the smoothed tensor field, $D(\boldsymbol{x})$, was numerically diagonalized by singular value decomposition at every grid point $\boldsymbol{x}_i$, resulting in three eigenvalues and eigenvectors (orientations modulo π) for every voxel. The field of eigenvectors corresponding to the largest

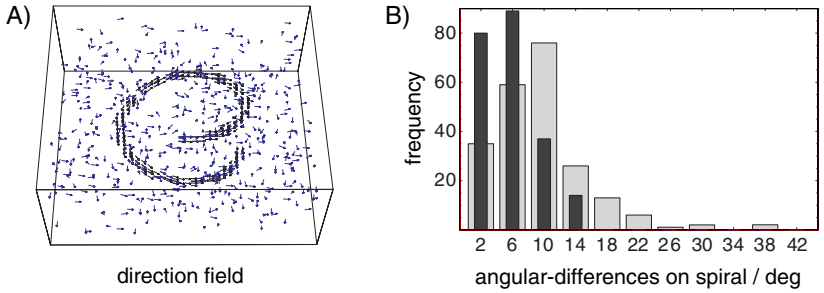

Fig. 4: Panel A shows a simulated direction field in space. In Panel B the distributions of angular differences are given: broad bars correspond to angles between uncorrupted and noisy directions on the spiral, small bars to angles between uncorrupted and smoothed directions. Total frequencies versus angle differences in degrees are given.

eigenvalue, $\hat{\boldsymbol{e}}(\boldsymbol{x}_i)$, gives the main direction field. In Fig. 4 the positive effect of smoothing on the main direction field is exemplified. Panel A illustrates the field around a simulated three-dimensional, anisotropic spiral tract embedded in an isotropic medium. Panel B shows the distributions of angular deviations from the ideal direction for voxels on the spiral.

As on the scale of the measured grid, the flow of axon bundles cannot be resolved completely, the regularization deals with averaged quantities. Correspondingly, in regions of crossing or merging axon directions cancellation is possible, leading to partial volume voxels with artificially low anisotropy. To introduce the direction information into these voxels, a rotation algorithm was developed, which proceeds essentially in two steps:

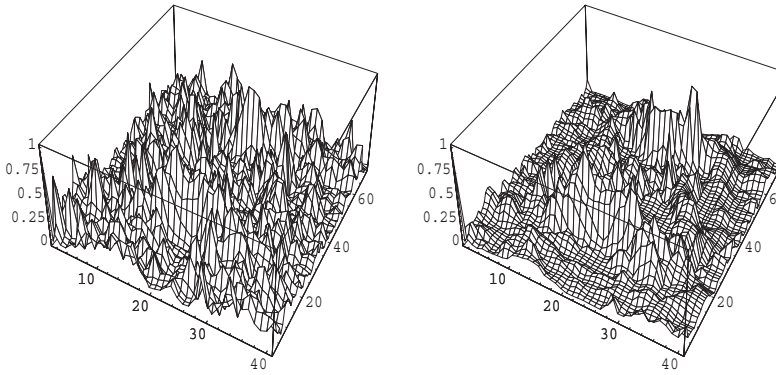

Fig. 5: The anisotropy coefficient $A_{\text{major}} \in [0, 1]$ for the axial region of Fig. 2; left: based on raw data, right: based on smoothed tensor field

1. According to the eigenvalues of the partial volume voxel, decide if the isotropy is two or three dimensional by the following procedure: Sort the eigenvalues in decreasing order and check if the first two or three eigenvalues are close (if the local tensor is disk shaped or spherical).
2. Then, two or three directions are mapped to this voxel by an algorithm which minimizes (modulo π) the mean angular deviation of a rotating vector to the main streams of directions in the neighborhood. In case of a two dimensional isotropy, the corresponding eigenvectors define the rotation plane of the vector, in case of three dimensions the rotation covers a sphere.

To model the direction of the axon bundles below the grid resolution, a local bilinear interpolation of the discrete direction field was performed, according to:

$$\hat{\boldsymbol{e}}(\boldsymbol{x}) = \sum_{\boldsymbol{x}_i \in 8-\text{neighborhood}(\boldsymbol{x})} \hat{\boldsymbol{e}}(\boldsymbol{x}_i) \cdot \left|1 - \frac{|x - x_i|}{\Delta x}\right| \cdot \left|1 - \frac{|y - y_i|}{\Delta y}\right| \cdot \left|1 - \frac{|z - z_i|}{\Delta z}\right| \quad , \tag{3}$$

where $\Delta x, \Delta y$, and Δz are the grid lengths.

If a partial volume voxel which includes several directions is in the 8-neighborhood, that direction which is closest to those of the neighboring standard voxels is chosen. The standard voxels have a cigar shaped tensor and are chosen by an anisotropy coefficient above a certain threshold. Anisotropy coefficients are strongly biased by noise, a review of recent coefficients and a discussion of their noise dependence is given in [2]. The effect of the presented regularization on the coefficient

$$A_{\text{major}} = \frac{\lambda_1 - (\lambda_2 + \lambda_3)/2}{\lambda_1 + \lambda_2 + \lambda_3} \qquad \text{for sorted eigenvalues} \quad \lambda_1 \geq \lambda_2 \geq \lambda_3 \tag{4}$$

is shown in Fig. 5, where the anisotropy for the raw data is compared to those of the smoothed tensor field, the region presented is the same as in Fig. 2.

On the basis of this interpolated direction field, tracks of axon bundles can be calculated as follows:

1. Choose the seed point of the track and the initial orientation via the nearest standard voxel.
2. Align the neighboring directions according to the initial orientation and calculate the interpolated direction by Eq. (3).
3. Proceed with a fixed step length Δs in this direction.
4. If the anisotropy is above the threshold, use the new position as seed point, the direction of step 3 to determine the initial orientation for the next iteration, and continue with step 2.

For $\Delta s \to 0$, this procedure essentially approaches an initial value problem for differential equations [4], according to this in step 3 a Runge-Kutta procedure gives more stable results. In Fig. 6 the direction field of the smoothed tensors is shown for 5 axial slices around the corpus callosum for $A_{\text{major}}^{\text{smoothed data}} \geq 0.3$. Several calculated tracks in are included.

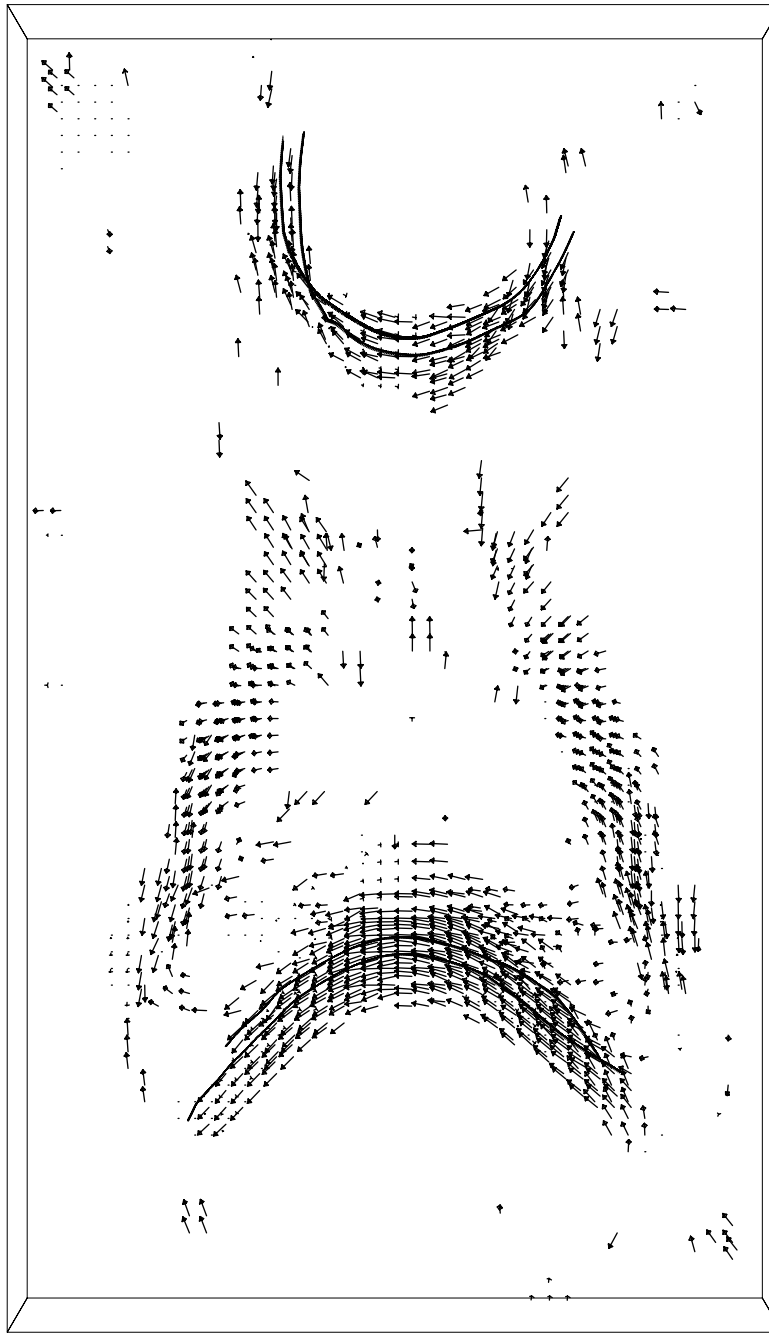

Fig. 6: The direction field around the corpus callosum as in Fig. 2 for 5 contiguous axial slices. Voxels for $A_{\text{major}} > 0.3$, based on the smoothed tensor field, are shown. Several calculated tracks are included

4 Conclusion

Spatially smoothing the tensor field is equivalent to a homogenization of the directions of the eigenvectors and of the eigenvalues which are derived by diagonalization. Therefore smoothing has an important impact on anisotropy coefficients and on tracking. For anatomical and geometrical reasons, the tensor field shows discontinuous patterns. In the corpus callosum region, anatomy gives rise to abrupt changes in the anisotropy signal from one voxel to the next. Similarly, for crossing or merging fiber tracks, the finite grid resolution can produce voxelwise changes in anisotropy or partial volume effects. Therefore, edge preserving smoothing is the method of choice to regularize diffusion signals or their tensor fields. The proposed tracking method was tested in model cases and by application to real data. Near the corpus callosum, where we found only standard voxels, reasonable results were achieved. Crossing and partial volume situations were up to now studied only by model simulations, more analyses are necessary to adapt the proposed method, which can handle only isolated, non-standard voxels, to realistic situations. The present tracking algorithm uses local information of the direction field only and proceeds in the frame of an initial value problem. To explore anatomical connectivity boundary value conditions which introduce anatomical knowledge about the starting and ending regions of the tracks should also be treatable. Furthermore, it seems to be experimentally evident that partial volume voxels with crossing tracks can also appear as groups or larger clusters in white matter [11]. For both reasons more global tracking methods than the present ones should additionally be applied. This could be achieved, e. g., by optimization methods of variational calculus which offer a flexible tool to combine global aspects with convenient priors.

Acknowledgment: We thank Dr. D. P. Auer for her kind interest and Dr. C. Gössl for providing us with the test example in Fig. 4. In addition, we would like to thank the referees for fruitful suggestions.

References

1. Pierpaoli C and Basser PJ. *Magn. Reson. Med.* **36** 893-906 (1996)
2. Skare S, Li TQ, Nordell B, and Ingvar M. *Magn. Reson. Imag.* **18** 659-669 (2000)
3. Parker GJM, Schnabel JA, Symms MR, et al. *J. Magn. Reson. Imag.* **11** 702-710 (2000)
4. Basser PJ, Pajevic S, Pierpaoli C, et al. *Magn. Reson. Med.* **44** 625-632 (2000)
5. Poupon C, Clark CA, Frouin V, et al. *NeuroImage* **12** 184-195 (2000)
6. Stejskal EO and Tanner JE. *J. Chem. Phys.* **42** 288-292 (1965)
7. Hahn K, Prigarin S, and Pütz B. *NeuroImage* **13** S142 (2001)
8. Aurich V and Weule J. Non-linear gaussian filters performing edge preserving diffusion. In *Proc. 17. DAGM-Symposium*, pages 538-545, Bielefeld, Springer (1995)
9. Henkelmann M. *Med. Phys.* **12** 232-233 (1985)
10. Winkler G, Aurich V, Hahn K, et al. *Pattern Recognition and Image Analysis* **9** 749-766 (1999)
11. Wiegell MR, Larsson HBW, and Wedeen VJ. *Radiology* **217** 897-903 (2000)